Hemiacetals of Acetophenone. Aromatic Substituent Effects in the H^+- and General-base-catalysed Decomposition in Aqueous Solution

Robert A. McClelland,*[a] Karen M. Engell,[b] Truels S. Larsen[b] and Poul E. Sørensen*[b]
[a] *Department of Chemistry, University of Toronto, Toronto, Ontario, Canada M5S 1A1*
[b] *Chemistry Department A, The Technical University of Denmark, DK-2800 Lyngby, Denmark*

We describe a double-mixing stopped-flow technique for the study of the acid- and base-catalysed breakdown of the unstable methyl hemiacetals of aryl-substituted acetophenones in aqueous solution. The approach takes advantage of the build-up of the hemiacetal during the H^+-catalysed decomposition of the corresponding dimethyl acetal. Thus, mixing a weakly basic solution of acetal with excess acid provides a solution containing unchanged acetal, the acetophenone product of the hydrolysis and the hemiacetal intermediate. After a short period of time (< 1 s) corresponding to the maximum build-up of hemiacetal, this solution is mixed with a neutral or weakly basic buffer solution. This second pH jump quenches the acetal hydrolysis, but not the hemiacetal breakdown. The kinetics of the hemiacetal can then be monitored spectrophotometrically. Twelve aryl-substituted acetophenone dimethyl acetals ranging from 4-dimethylamino to 3-bromo were synthesised and investigated. Hammett ρ values for the H^+-catalysed acetal and hemiacetal breakdown are in good agreement with literature data, but our analysis suggests a larger resonance effect component than previously assumed. The corresponding set of Hammett plots for base catalysis of hemiacetal breakdown reveals a relatively weak dependence of the catalytic constants on aromatic substitution, which appears to be inconsistent with much stronger dependences on substitution in the leaving alcohol. We propose a case of non-perfect synchronization or imbalance in the transition state where, in the breakdown direction in a class n mechanism, the degree of C–O bond breakage as measured by β_{lg} is considerable, but the change in hybridization of the central carbon ($sp^3 \longrightarrow sp^2$), as measured by ρ, lags behind in the transition state so that there is less interaction with the aromatic substituents here.

The detailed nature of the complex mechanisms of acid–base catalysis in aqueous media has been the subject of many important studies. Hydrate and hemiacetal decomposition reactions have provided useful information about the manner in which substituent changes effect reactivity. This information is relevant to a large number of acid–base-catalysed reactions in organic chemistry, and is also important in the understanding of many reactions catalysed by enzymes.

We present here evidence that in some cases *acetals* can serve as excellent precursors for hemiacetals that would otherwise be difficult to obtain.

The hydrolysis of acetals is now well established to proceed in three reaction stages involving the formation of oxocarbocation and hemiacetal intermediates (Scheme 1).[1]

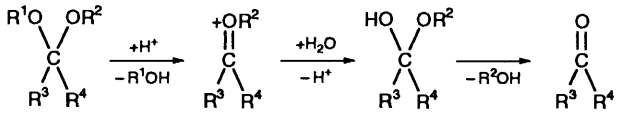

Scheme 1

The second stage, the hydration of the oxocarbocation, is generally very rapid, especially for ions such as those involved in the hydrolysis of simple acetals.[2] Although in the early literature it was usually assumed that the first stage was rate-limiting,[1] there are now several examples where the third stage has a similar rate or is even slower. In such a case the third stage is partially or wholly rate-limiting in the formation of the carbonyl product of the hydrolysis, and the hemiacetal intermediate actually accumulates during the reaction. This situation has been most dramatically demonstrated for mixed acetals where there is a significant difference between the leaving groups in the first and third stages. Examples include systems where the first stage is accelerated relative to the third because of the presence of a good leaving group,[3] intramolecular catalysis,[4] or relief of ring strain,[5] and where the third stage is slowed since it involves opening of a ring while the first involves loss of an exocyclic group.[6] An example in a symmetrical acetal is the di-*tert*-butyl acetal of benzaldehyde where the first stage is significantly accelerated relative to the third because of relief of steric strain.[7] Each of these examples, under certain conditions, has a third stage that is actually significantly slower than the first. For symmetrical dimethyl and diethyl acetals it would appear in general that the third stage is always faster. However, with benzaldehyde derivatives, it has been known for some time that the rates are still sufficiently close for a small, but detectable, amount of hemiacetal to accumulate during the acetal hydrolysis.[8,9] We have recently provided in preliminary form the details of experiments using a multi-mixing stopped-flow technique that demonstrates that the same situation holds for the dimethyl acetal of acetophenone.[10] In this paper we provide further details of this procedure, as well as demonstrate its application to acetals of ring-substituted acetophenones, with substituents varying from 4-dimethylamino to 4-bromo. The multi-mixing technique has the feature of providing fairly accurate kinetic data for the base-catalysed decomposition of the hemiacetal. The data that we have obtained in this context are discussed in the context of previous results obtained for hemiacetal decomposition. The acetophenone hemiacetals have the feature of being relatively unstable compared with derivatives that have previously been studied.

Experimental and Results

Materials.—Twelve aryl-substituted dimethyl acetals of

acetophenone were synthesised according to the following general procedure (Scheme 2).[11] Acetophenone (0.10 mol) was dissolved in a mixture of trimethyl orthoformate (0.11 mol) and 20–30 cm^3 of dry methanol. 2–3 drops of conc. sulfuric acid

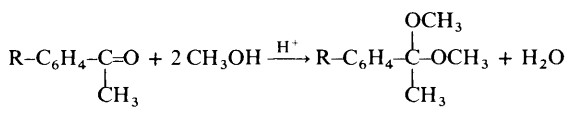

$$HC(OCH_3)_3 + 3\,H_2O \longrightarrow 3\,CH_3OH + HCOOH$$

Scheme 2

were added and the flask was stoppered and sealed with Parafilm. The mixture was left at ambient temperature for 3 days to react. The acid was then neutralized over 24 h by adding an excess of anhydrous sodium carbonate and the solvent was removed under reduced pressure. The remaining rather viscous liquid was then fractionally distilled under vacuum in a spinning band column, the middle fraction (*ca.* 5 cm^3) was kept and stored over anhydrous sodium carbonate at 4 °C.

Acetophenones, apart from the 4-dimethylamino compound, were all commercial and were used without further purification in the synthesis.

Product identification for the various acetals is given below. ^1H NMR spectra were run on a Bruker AD-250 instrument at 250 MHz. Signals are referenced to internal Me_4Si.

The methyl acetal of aryl-substituted acetophenones reported below have all been synthesised before in a number of different contexts.[2a,11d,12,13] They are easily identified by ^1H NMR spectroscopy. Two distinct signals (singlets) appear almost independently of the substituent: $\delta(CDCl_3) \approx 1.52$ (3 H, s, Me) and ≈ 3.20 (6 H, s, OMe).[12c,13b] The identity of the aromatic group was confirmed by its NMR signal and, following Young and Jencks,[2a] by observing the UV spectrum of the product of acetal hydrolysis. This spectrum was always in good agreement with that for the corresponding ketone, to within experimental error.

Acetophenone dimethyl acetal (1,1-*dimethoxy*-1-*phenylethane*). B.p. 90–91 °C at 19 Torr (lit.,[12c,b,13b] b.p. 66 °C at 5.8 Torr, 90 °C at 20 Torr, 68–69 °C at 6 Torr); $\delta_H(CDCl_3)$ 1.52 (3 H, s, Me), 3.22 (6 H, s, OMe), 7.2–7.6 (5 H, m, ArH) in good agreement with literature reports;[12c,13b] $\lambda_{max}(H_2O)$/nm 245.9 and 285 [lit., [14] λ_{max}(MeOH)/nm 240 and 278.5].

4-*Methoxyacetophenone dimethyl acetal* [1,1-*dimethoxy*-1-(4-*methoxyphenyl*)*ethane*]. B.p. 144–146 °C at 32 Torr (lit.,[12c,13b] b.p. 64 °C at 0.15 Torr, 99–100 °C at 5 Torr); $\delta_H(CDCl_3)$ 1.52 (3 H, s, Me), 3.17 (6 H, s, OMe), 3.80 (3 H, s, ArOMe), 6.86 (2 H, br d, half of AB system, 2 × ArH) and 7.40 (2 H, br d, half of AB system, 2 × ArH) [lit.,[13b] $\delta_H(CCl_4)$ 1.47, 3.13, 3.78 and 6.8–7.53, respectively]; $\lambda_{max}(H_2O)$/nm 218.2 and 277.6 [lit.,[14] λ_{max}(MeOH)/nm 217 and 270].

4-*Methylacetophenone dimethyl acetal* [1,1-*dimethoxy*-1-(4-*methylphenyl*)*ethane*], b.p. 107 °C at 19 Torr (lit.,[12c,13b] b.p. 78 °C at 5.8 Torr, 80–81 °C at 6 Torr); $\delta_H(CDCl_3)$ 1.52 (3 H, s, Me), 3.17 (6 H, s, OMe), 2.34 (3 H, s, ArMe), 7.0–7.3 (2 H, br d, half of AB system, 2 × ArH) and 7.6–7.8 (2 H, br d, half of AB system, 2 × ArH) [lit.,[13b] $\delta_H(CCl_4)$ 1.47, 3.10, 2.30 and 7.0–7.45, respectively]; $\lambda_{max}(H_2O)$/nm 257.1 [lit.,[14] λ_{max}(MeOH)/nm 252].

3-*Methylacetophenone dimethyl acetal* [1,1-*dimethoxy*-1-(3-*methylphenyl*)*ethane*]. B.p. 118–119 °C at 29 Torr, $\delta_H(CDCl_3)$ 1.53 (3 H, s, Me), 2.38 (3 H, s, ArMe) 3.19 (6 H, s, OMe) and 7.0–7.4 (4 H, m, ArH); $\lambda_{max}(H_2O)$/nm 249.7 and 294.4 [lit.,[14] λ_{max}(MeOH)/nm 245 and 287].

4-*Fluoroacetophenone dimethyl acetal* [1,1-*dimethoxy*-1-(4-*fluorophenyl*)*ethane*]. B.p. 94–96 °C at 32 Torr (lit.,[13b] b.p. 62–63 °C at 5 Torr); $\delta_H(CDCl_3)$ 1.54 (3 H, s, Me), 3.18 (6 H, s, OMe) and 7.0–7.5 (4 H, m, ArH) [lit.,[13b] $\delta_H(CCl_4)$ 1.48, 3.13 and 6.9–7.68, respectively]; $\lambda_{max}(H_2O)$/nm 248.8 [lit.,[14] λ_{max}(MeOH)/nm 242].

3-*Methoxyacetophenone dimethyl acetal* [1,1-*dimethoxy*-1-(3-*methoxyphenyl*)*ethane*]. B.p. 140–143 °C at 35 Torr, $\delta_H(CDCl_3)$ 1.53 (3 H, s, Me), 3.20 (6 H, s, OMe), 3.83 (3 H, s, ArOMe) and 6.8–7.3 (4 H, m, ArH); $\lambda_{max}(H_2O)$/nm 217.5, 251.4 and 308.8 [lit.,[14] λ_{max}(MeOH) 216.5, 246 and 305].

4-*Chloroacetophenone dimethyl acetal* [1,1-*dimethoxy*-1-(4-*chlorophenyl*)*ethane*]. B.p. 120–121 °C at 19 Torr (lit.,[12c,13b] b.p. 56–75 °C at 0.3 Torr, 93–94 °C at 5 Torr); $\delta_H(CDCl_3)$ 1.54 (3 H, s, Me), 3.18 (6 H, s, OMe), 7.3–7.5 (2 H, br d, half of AB system, 2 × ArH), 7.7–7.9 (2 H, br d, half of AB system, 2 × ArH) [lit.,[13b] $\delta_H(CCl_4)$ 1.48, 3.15 and 7.4–7.45, respectively]; $\lambda_{max}(H_2O)$/nm 255.6 [lit.,[14] λ_{max}(MeOH)/nm 250 nm].

4-*Bromoacetophenone dimethyl acetal* [1,1-*dimethoxy*-1-(4-*bromophenyl*)*ethane*]. B.p. 145–148 °C at 32 Torr, $\delta_H(CDCl_3)$ 1.52 (3 H, s, Me), 3.18 (6 H, s, OMe) and 7.4–7.9 (4 H, m, ArH); $\lambda_{max}(H_2O)$/nm 259.5 [lit.,[14] λ_{max}(MeOH)/nm 254 nm].

3-*Bromoacetophenone dimethyl acetal* [1,1-*dimethoxy*-1-(3-*bromophenyl*)*ethane*]. B.p. 142–143 °C at 30 Torr, $\delta_H(CDCl_3)$ 1.52 (3 H, s, Me), 3.18 (6 H, s, OMe) and 7.2–7.7 (4 H, m, ArH); $\lambda_{max}(H_2O)$/nm 246.3 and 297.3 [lit.,[14] λ_{max}(MeOH)/nm 240.5 and 287 nm].

We were not able to isolate the dimethyl acetals of the three less reactive acetophenones, R = 4-dimethylamino, 4-amino and 4-hydroxy, since they clearly form an equilibrium with the starting material which is well over to the left-hand side. This is a well-known situation for acetals of ketones,[11a,13a] the thermodynamics of their equilibria depending on a number of parameters. We did not try to study these systems in detail. The acidic methanolic solutions were protected from moisture and stored at 4 °C. They were used directly as stock solutions of the acetal in the preparation of the basic aqueous solutions for the kinetic stopped-flow experiments (*vide infra*). Apart from a high background absorption from unchanged acetophenone the kinetic behaviour of these solutions was as expected.

A synthetic procedure for making 4-dimethylaminoacetophenone has been reported by Lienhard *et al.*[15] Commercial 4-aminoacetophenone (15 g) was placed in a 500 cm^3 round-bottomed flask to which were added 30 cm^3 of methyl iodide, 75 g of sodium carbonate decahydrate and 50 cm^3 of distilled water. The mixture was heated and refluxed for 18 h at 95 °C. A light brown solid was formed after a few hours. After being cooled the mixture was neutralized with HCl and the precipitate was filtered off. This substance (salt) consisting of the iodide of 4-trimethylammonium–acetophenone was then dried at 240 °C for several hours to drive off one molecule of methyl iodide per molecule of substrate. After being dried, the solid was taken up in light petroleum (b.p. 60–80 °C) and the product recrystallized several times from the same solvent. The first extraction gave 2.57 g of a yellowish green product, m.p. 103–106 °C (lit.,[15] 105 °C). This m.p. is close to that for the starting material (lit.,[16] 105.5 °C). The identification was therefore supplemented by ^1H NMR and UV data, $\delta_H(CDCl_3)$ 2.51 (3 H, s, Me), 3.08 (6 H, s, NMe_2), 6.65 (2 H, br d, half of AB system, 2 × ArH) and 7.89 (2 H, br d, half of AB system, 2 × ArH), as compared with $\delta_H(CDCl_3)$ 2.52, 3.09, 6.71 and 7.95, respectively;[14] $\lambda_{max}(H_2O)$/nm 239.9 and 334.9 [lit.,[14] λ_{max}(MeOH)/nm 236 and 332.5].

Other chemicals were high grade commercial products, used without further purification. Millipore-Q water was used throughout.

H^+-*Catalysis*.—Kinetic experiments were carried out follow-

Table 1 Summary of data for the H^+-catalysed decomposition of some *meta*- and *para*-substituted acetophenone dimethyl acetals[a]

acetal $\xrightarrow{k_1}$ hemiacetal $\xrightarrow{k_2}$ acetophenone

	Hammett sigma		Acetal		Hemiacetal	
Substituent	σ	σ^+	k_H/dm^3 mol^{-1} s^{-1}	k_w/s^{-1}	k_H/dm^3 mol^{-1} s^{-1}	k_w/s^{-1}
4-Dimethylamino	−0.63	−1.7	1.47×10^5	0.0009	—	—
4-Amino	−0.57	−1.3	4.91×10^4	0.0014	—	—
4-Hydroxy	−0.37	−0.92	2.83×10^4	0.000	—	—
4-Methoxy	−0.268	−0.78	9.40×10^3	−0.025	1.82×10^5	−185
4-Methyl	−0.17	−0.31	2.09×10^3	0.52	3.37×10^4	14
3-Methyl	−0.69	−0.066	1.68×10^3	0.033	2.35×10^4	−10
Parent	0	0	9.56×10^2	0.133	1.96×10^4	−24
4-Fluoro	0.062	−0.07	1.19×10^3	0.015	1.44×10^4	−0.80
3-Methoxy	0.115	0.047	4.53×10^2	0.013	7.32×10^3	5.8
4-Chloro	0.227	0.114	4.07×10^2	0.020	7.15×10^3	1.26
4-Bromo	0.232	0.15	3.79×10^2	−0.025	6.23×10^3	7.8
3-Bromo	0.391	0.405	1.56×10^2	−0.003	3.78×10^3	0.04

[a] T = 25 °C, I = 1.0 mol dm^{-3}.

ing the appearance of the ketone products at their absorption maxima in the range 240–340 nm. Addition of the acetophenone acetals to acetate buffers of pH 4.6–5.6 (conventional thermostatted double-beam Shimadzu UV-150-02 spectrophotometer) resulted in absorbance increases that followed excellent first-order kinetics. The observed first-order rate constants do not vary significantly with the concentration of buffer in experiments at constant pH (Table S1),* but they are proportional to H^+ concentration. In solutions of this pH, the first reaction stage (Scheme 1) is entirely rate-limiting in the formation of the product. This situation arises since this stage proceeds with H^+-catalysis, while the third stage is efficiently catalysed by hydroxide ion, a point that will be unambiguously established later. Thus the observed rate constants represent the specific acid-catalysed conversion of the acetal to the oxocarbocation. Primary kinetic data for this process are given in Table S1* and the resulting values of the H^+-catalytic coefficients are collected in Table 1.

Experiments were also conducted by mixing, in the stopped-flow apparatus (HiTech Scientific PQ/SF-53 instrument in the single-mixing mode), a dilute base solution (2 mmol dm^{-3} NaOH) of the acetal with an excess of HCl. In contrast with the situation at higher pH, strict adherance to exponential kinetics is not observed, the absorbance change exhibiting a slight lag in its increase in the initial part of the reaction. This behaviour is similar to that observed previously for benzaldehyde acetals,[8] and is characteristic of the formation of the product in a kinetic system consisting of two consecutive first-order reactions the rate constants of which are not substantially different (Scheme 3).

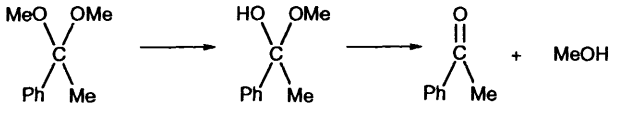

Scheme 3

A double exponential equation describes this situation,[17] with the two exponents equal to the first-order rate constants for the two reactions. Such an equation does indeed provide an excellent fit to the experimental data (data processed by OLIS software[18]). The two rate constants differ by a factor of about ten for each acetal. Primary kinetic results from this series of experiments are also presented in Table S1* and the final (derived) H^+-catalytic coefficients for both acetal and hemiacetal breakdown are given in Table 1. The kinetic data for acetal breakdown in Table 1 are therefore the combined results from two different sources.

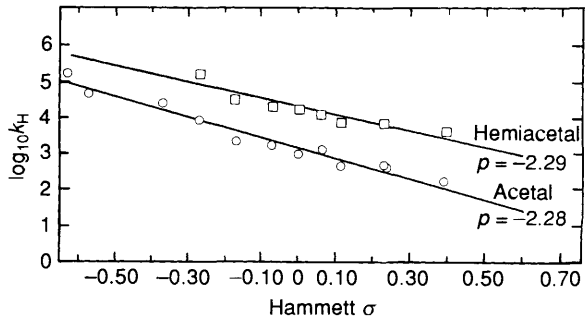

Fig. 1 Hammett plots for the H^+-catalysed breakdown of a series of aryl-substituted acetophenone dimethyl acetals and methyl hemiacetals; data taken from Table 1

The ratio k_H(acetal)/k_H(hemiacetal) is somewhat dependent on the substituent on the aromatic moiety, becoming smaller with increased electron donation. On variation of the pH, both rate constants are seen to be proportional in H^+-concentration, providing two catalytic coefficients in H^+. The smaller of these is, to within experimental error, the same as the value of k_H obtained in the phosphate buffers, and can therefore be assigned to H^+-catalysis of the first reaction stage. The larger rate constant therefore corresponds to H^+-catalysis of the decomposition of the hemiacetal. The aromatic substituent effects on k_H are best shown in a Hammett plot (Fig. 1).

Thus, for acetophenone dimethyl acetals, H^+-catalysis of the hemiacetal breakdown occurs about an order of magnitude faster than the conversion of the acetal into oxocarbocation. A similar difference is observed for analogous benzaldehyde acetals.[8] The substituent effect in the two series is also similar, with the two rates becoming closer for electron-donating substituents.

With such a situation, the hemiacetal is predicted to accumulate to a small extent during the hydrolysis of the acetal under acidic conditions, rising to a maximum of 5–7% of the initial concentration of the acetal. This will be verified further in the following section.

Table 1 also contains (intercept) values for water catalysis. These values are uncertain and, in general, indistinguishable from zero, in accordance with the experimental fact that acetal

* Supplementary tables (S1 and S2) have been deposited with the British Library, Sup. No. 57031 (40 pp.) For details of the supplementary publications scheme, see 'Instructions for Authors (1994)', *J. Chem. Soc., Perkin Trans. 2*, 1994, issue 1.

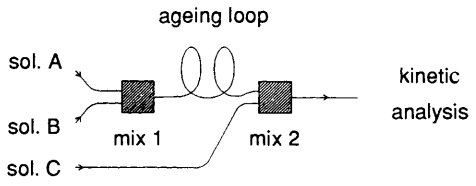

Fig. 2 An illustration of the principle of double-mixing stopped-flow measurements

hydrolysis is generally specific-acid catalysed[19] and that aromatic hemiacetals decompose with very small or undetectable water catalytic rate constants.[20]

Base Catalysis.—In this experimental series we took advantage of a stopped-flow double-mixing technique (Hi-Tech Scientific PQ/SF-53 instrument), the principle of which is illustrated in Fig. 2. The solution resulting from mixing of solutions A and B can be aged either by interrupting the flow of liquid for a certain preset time (interrupt mode) or by varying the length of the loop (or the flow rate) between the two mixing chambers in a continuous mode experiment. The aged solution is then mixed (quenched) with solution C in the second mixing chamber and the resulting mixture is analysed kinetically as in an ordinary stopped-flow experiment.

Mixing of an aqueous solution of the acetal in base (0.002 mol dm^{-3} NaOH) with an excess of acid (0.004 mol dm^{-3} HCl) in the first mixing chamber initiated acetal hydrolysis in the loop, causing the concentration of hemiacetal to build up. When the maximum concentration of hemiacetal was reached, the second mixing in chamber 2 was effected, where the pH of the acetal and hemiacetal containing solution was raised by a buffer. The result was instantaneous quenching of further acetal hydrolysis, and the kinetic fate of the hemiacetal was followed spectrophotometrically at the wavelength for maximum absorption of the free acetophenone.

A knowledge of the most ideal delay time between mix 1 and 2 in the type of experiment described above requires a systematic investigation in which the total absorption change for observed hemiacetal breakdown is followed as a function of the (interrupt) delay time. The time of maximum hemiacetal build-up (5–7% after $\approx$ 0.3 s) will vary somewhat with experimental conditions and with the aryl substituent, but in general we were able to use the same loop length, corresponding to 0.2–0.6 s time delay in a continuous-mode experiment for all the substances in the series.

In the following we describe the results of the buffer-catalysed breakdown studies of the whole series of dimethyl acetals of aryl-substituted hemiacetals, carried out by following spectrophotometrically the absorbance change *vs.* time after the second mixing as described above. Excellent first-order kinetic traces were observed with a drifting infinity line. Such behaviour can be described by eqn. (1).

$$\Delta A = A_1\exp(-k_1t) + A_2k_2t + A_3 \qquad (1)$$

The first-order rate constant k_1 is for the (faster) hemiacetal breakdown, and the zero-order rate constant k_2 is for a constant (slow background) breakdown of acetal, which cannot be quenched completely at the actual pH. This slow background reaction approaches zero-order since it constitutes only a very small part of the normal first-order trace for acetal breakdown (step 1 in Scheme 1). A drifting infinity line was observed for all the compounds studied, its degree of importance varying with pH and substituent. In all cases it is easily accounted for by eqn. (1), which was used throughout as a fitting model for the OLIS data processing software.[18]

Primary data from the investigation of the series of acetophenones substituted in the benzene ring in a number of buffers are listed in Table S2.

The usual expression for treating catalytic data in general acid–base catalysis is given as eqn. (2) for a single buffer system,

$$k_{obs} = k_w + k_H[H^+] + k_{OH}[OH^-] + \{(1 - r)k_A + rk_{HA}\}([HA] + [A^-]) \qquad (2)$$

where k_{obs} is the observed first-order rate constant; k_w, k_H and k_{OH} are the water-related catalytic constants; k_{HA} and k_A are the catalytic constants for the two buffer components, respectively. The independent variables are $[H^+]$, $[OH^-]$ (pH), $r = [HA]/([HA] + [A^-])$ = fraction of acid in buffer, and $[HA] + [A^-]$ = total buffer concentration. Thus, k_{obs} depends on a number of parameters and a good deal of systematic experimental work in combination with graphical methods is usually required to determine all constants for a given reaction.

We have solved this problem for all the primary data in Table S2 by making use of a (commercial) program (MINSQ II[21]) for nonlinear curve fitting and parameter estimation on a microcomputer. In accordance with eqn. (2), the model for fitting takes the form $Y = KA + KB \times 10^{(X-14)} + [(1 - R) \times KC + R \times KD] \times Z$, where X = pH, $R = r$ and $Z = [HA] + [A^-]$ are the independent variables. $KA = k_w + k_H[H^+]$, $KB = k_{OH}$, $KC = k_A$ and $KD = k_{HA}$ are the various catalytic constants to be estimated.

Since all the primary data in Table S2 were obtained at pH > 6 and since k_w and k_{HA} are in general negligible compared with the observed contributions from base catalysis in this region,[20] KA and KD in the model expression are negligible for all the systems studied, in accordance with the fact that the best fits were obtained when these constants were fixed equal to zero in the program. The populations of data are, in general, too small to allow all four constants to be estimated, but in a few (successful) cases, the constants KA and KD would always come out as relatively small positive or negative values. A further implication of this fact is that eqn. (2) may then be reduced to eqn. (3), which states that a plot of $k_{obs}/[OH^-]$ *vs.* $[A^-]/[OH^-]$

$$k_{obs}/[OH^-] = k_{OH} + k_A[A^-]/[OH^-] \qquad (3)$$

should be linear and provide us with k_{OH} and k_A as intercept and slope, respectively. We did apply this (classical) method to several of the data sets in Table S2 and found complete agreement of the results with those from the above data-fitting procedure.

As an illustration, Table 2 contains observed and calculated first-order rate constants for the phosphate-catalysed (parent) hemiacetal breakdown reactions as well as the catalytic constants estimated from the MINSQ fitting procedure. Standard deviations and regression coefficients are available for sufficiently large populations of data. Remaining observed and calculated data are given in Table S2.

All calculated catalytic constants are collected in Table 3.

Discussion

Acid Catalysis.—Our experimental results for the specific-acid-catalysed hydrolysis of acetophenone acetals are directly comparable and agree well with the data reported by Young and Jencks,[2a] with our data covering a somewhat larger σ range. The hemiacetal results have not been determined for this series before. The Hammett plots in Fig. 1 are based on classical σ values (Table 1) and we have chosen to draw straight lines through both sets of data since we were not immediately able to detect (visually) any deviation from linearity, within experimental error. We found from the slopes $\rho = -2.88 \pm 0.17$,

Table 2 Kinetic data for the decomposition of parent acetophenone dimethyl acetal catalysed by phosphate buffer[a]

acetal $\xrightarrow{k_1}$ hemiacetal $\xrightarrow{k_2}$ acetophenone

$[Buffer]_{tot}$/mol dm^{-3}	pH	k_2/s^{-1} (obs)[b]	k_2/s^{-1} (calc)[c]
$r = 0.1118$			
0.0356	7.49	5.32 ± 0.16	5.16
0.071	7.60	6.89 ± 0.09	6.90
0.108	7.65	8.14 ± 0.13	8.02
0.143	7.69	9.26 ± 0.06	9.04
0.179	7.73	10.36 ± 0.06	10.13
$r = 0.250$			
0.0533	6.93	1.88 ± 0.01	1.77
0.1067	6.97	2.48 ± 0.01	2.34
0.160	6.99	3.09 ± 0.04	2.86
0.2133	7.00	3.69 ± 0.03	3.34
0.2667	7.02	4.31 ± 0.04	3.86
0.040	7.16	2.29 ± 0.02	2.58
0.080	7.22	2.86 ± 0.02	3.25
0.120	7.25	3.30 ± 0.02	3.77
0.160	7.27	3.83 ± 0.11	4.24
0.200	7.30	4.26 ± 0.08	4.78
$r = 0.400$			
0.050	6.71	0.961 ± 0.013	1.13
0.100	6.76	1.33 ± 0.02	1.57
0.150	6.77	1.61 ± 0.01	1.92
0.200	6.77	1.88 ± 0.01	2.26
0.250	6.78	2.13 ± 0.01	2.61
$r = 0.500$			
0.067	6.46	0.912 ± 0.014	0.823
0.134	6.46	1.33 ± 0.01	1.20
0.200	6.48	1.75 ± 0.04	1.59
0.266	6.50	2.19 ± 0.02	1.98
0.334	6.50	2.63 ± 0.03	2.36

[a] $T = 25$ °C, $I = 1.0$, r = fraction of acid = [HA]/([HA] + [A$^-$]). Parent $\lambda_{max} = 255$ nm. [b] Mean values from primary data in Table S2. [c] Based on a MINSQ least squares procedure (see the text): $KA = k_w = 0.0$ s^{-1} (fixed), $KB = k_{OH} = (1.56 \pm 0.06) \times 10^7$ dm^3 mol^{-1} s^{-1}; $KC = k_A = (11.15 \pm 1.93)$ dm^3 mol^{-1} s^{-1}, $KD = k_{HA} = 0.0$ dm^3 mol^{-1} s^{-1} (fixed). Correlation coefficient = 0.993.

correlation coefficient = 0.982, and $\rho = -2.29 \pm 0.30$, correlation coefficient = 0.943, for acetal and hemiacetal, respectively. Our value of $\rho = -2.3$ for hemiacetal hydrolysis is consistent with $\rho = -2.2$ found for the H^+-catalysed breakdown of methyl acetals of 4-substituted α-bromoacetophenone,[20c] but our value of $\rho = -2.9$ for acetal hydrolysis compares poorly with $\rho = -2.2$ found by Young and Jencks under the same experimental conditions.[2a] However, this may be an artificial difference because a closer inspection of our Hammett plots shows that they both exhibit a weak upward curvature, *i.e.*, show positive deviation for the points deriving from the more electron-donating substituents. As a matter of fact, if we leave out the three points for the hydroxy and the two amino groups, a value of $\rho = -2.4$ (correlation coefficient = 0.964) is obtained.

At this stage we are faced with the classical dilemma of having to choose the 'best' Hammett substituent constants,[22] *i.e.*, either (1) denying that Hammett plots should show curvature and therefore treating Hammett σ as a statistical, adjustable parameter to linearize and to minimize deviations, or (2) stick to Hammett's classical σ values and try to explain observed deviations as special electronic effects or due to mechanistic details. A kind of compromise deals with separating observed substituent effects in polar (inductive) and reasonance (mesomeric) contributions as described by the multiple LFER expression shown in eqn. (4).[22]

$$\log (k/k_0) = \rho_I\sigma_I + \rho_R\sigma_R \quad (4)$$

One version of eqn. (4) is the Yukawa and Tsuno expression, $\log (k/k_0) = \rho[\sigma + r(\sigma^+ - \sigma)]$,[23] which shares the observed substituent effects between polar (σ) and resonance (σ^+) contributions, regulated by the parameter r. Young and Jencks[2a] found that their data for acetal hydrolysis were even better described by this equation, giving $\rho = -2.0$ for $r = 0.18$ and in good agreement with the results of a previously reported set of experimental data by Louden and Berke,[24] giving $\rho = -2.29$ for $r = 0.13$ under slightly different experimental conditions (5% dioxane, 30 °C). We have applied the Yukawa–Tsuno equation (curve fitting by MINSQII[21]) to our data for both acetal and hemiacetal hydrolysis. The following results were obtained: acetal, $\rho = -2.05 \pm 0.24$, $r = 0.42 \pm 0.15$, correlation coefficient = 0.994; hemiacetal, $\rho = -1.83 \pm 0.25$, $r = 0.53 \pm 0.23$, correlation coefficient = 0.979. The agreement between our result for acetal and that obtained by Young and Jencks[2a] is again seen to be good, apart from obvious differences in r. However, taking into account the general uncertainty of r, it cannot be excluded that this parameter, and thereby the importance of resonance effects, has been underestimated in the earlier work.[2a] Our set of data covers a wider range of σ values, including points for substituents where resonance plays an important role.

Young and Jencks[2a] have suggested a version of eqn. (4) where the contributions from polar and resonance effects are separated according to $\log (k/k_0) = \rho\sigma^n + \rho'(\sigma^+ - \sigma^n)$. This equation is transformed into the Yukawa–Tsuno equation if $\sigma^n = \sigma$ and $\rho^r = r\rho$. The parameter σ^n indicates the 'normal', purely polar (inductive) substituent constants given by van Bekkum *et al.* and by Taft.[25,22] According to this equation, Young and Jencks found, for the hydrolysis of acetophenone acetals, that the rate constants are satisfactorily correlated by $\rho = -2.0$ and $\rho^r = -0.7$. The corresponding values calculated for our set of data are $\rho = -2.29 \pm 0.25$ and $\rho^r = -1.13 \pm 0.09$ (correlation coefficient = 0.993). Again, as expected, our r value of 0.49 (1.13/2.29) is greater than $r = 0.35$ (0.7/2.0) from the work of Young and Jencks.[2a]

Base Catalysis.—The Hammett plots for the base-catalysed *hemiacetal* decomposition (data taken from Table 3) are shown in Fig. 3 for the various catalysts. The σ^+ scale is used simply because this scale gives the best straight lines through the points (ρ values are given in the plot). It is tempting here also to apply the Young and Jencks version[2a] of the Yukawa–Tsuno equation to obtain a weighting between polar and resonance effects. This was done only for hydroxide and phosphate as catalysts and the following results were obtained: hydroxide, $\rho = 0.40 \pm 0.25$ and $\rho^r = -0.46 \pm 0.08$ (correlation coefficient = 0.920); phosphate, $\rho = 0.27 \pm 0.16$ and $\rho^r = -0.38 \pm 0.04$ (correlation coefficient = 0.956). The corresponding (numerical) r values are 1.15 and 1.40, respectively, indicating a considerable contribution from resonance. However, the uncertainties of these numbers are too big for any firm conclusion to be drawn from them. This is closely related to the (limited) quality and scarcity of the experimental data, and at this point we conclude only that the sensitivity of the catalytic constants to aromatic substitution is quite small. Similar (small) ρ values were found for the breakdown of the methyl hemiacetals of 4-substituted α-bromoacetophenones: ρ(hydroxide) = −0.4, ρ(acetate) = +0.1, $\rho(H_2O) = +0.6$.[20c] The magnitude and signs of all these values are also in good agreement with data found for the breakdown of ethyl hemiacetals of benzaldehydes under slightly different experimental conditions ($I = 0.10$, 30 °C).[20d]

A Brønsted plot for base catalysis of the hemiacetal decomposition is seen in Fig. 4 (data taken from Table 3). The

Table 3 Collected catalytic constants for the base-catalysed decomposition of some *meta*- and *para*-substituted acetophenone methyl hemiacetals

Substituent	Hammett		Catalyst															
			Acetate $pK_A = 4.65$[a] $p,q = 1,2$[b]		Malonate $pK = 5.00$[a] $p,q = 1,4$[b]		Cacodylate $pK_A = 6.29$[a] $p,q = 1,2$[b]		Phosphate $pK_A = 6.49$[a] $p,q = 2,3$[b]		Methyl phosphonate $pK_A = 7.40$[a] $p,q = 1,3$[b]		TRIS[e] $pK_A = 8.36$[a] $p,q = 3,1$[b]		Borate $pK_A = 9.10$[a] $p,q = 3,4$[b]		Ammonia $pK_A = 9.54$[a] $p,q = 4,1$[b]		Hydroxide $pK_A = 15.74$[a] $p,q = 2,1$[b]
	σ	σ^+	k_A[c]	k_{OH}[d]	k_A[c]	k_{OH}[d]	k_A[c]	k_{OH}[d]	k_A[c]	k_{OH}[d]	k_A[c]	k_{OH}[d]	k_A[c]	k_{OH}[d]	k_A[c]	k_{OH}[d]	k_A[c]	k_{OH}[d]	k_{OH}[d,g]
4-Dimethylamino	−0.63	−1.7	—	—	—	—	—	—	40[f]	7.60	—	—	—	—	—	—	—	—	7.6
4-Amino	−0.57	−1.3	—	—	—	—	—	—	36.9	2.53	—	—	—	—	—	—	—	—	2.5
4-Hydroxy	−0.37	−0.92	—	—	—	—	—	—	22.3	3.26	—	—	—	—	—	—	—	—	3.3
4-Methoxy	−0.268	−0.78	—	—	0.33	2.58	2.70	2.60	17.1	5.39	19.3	2.35	58.9	2.10	—	—	—	—	3.0
4-Methyl	−0.17	−0.31	—	—	—	—	2.30	1.80	14.6	1.78	18.6	1.40	54.8	1.55	—	—	—	—	1.6
3-Methyl	−0.07	−0.066	—	—	—	—	2.76	1.20	11.6	1.80	16.7	1.01	40.0	0.88	—	—	—	—	1.2
Parent	0.00	0.00	⩽0.3[f]	1.04	—	—	2.75	1.45	11.2	1.56	15.8	1.28	49.1	1.19	250	0.96	717	1.06	1.2
4-Fluoro	0.062	−0.07	—	—	—	—	5.13	2.17	16.3	2.52	23.5	1.93	—	—	—	—	—	—	2.2
3-Methoxy	0.115	0.047	—	—	0.3[f]	2.13	3.48	1.22	11.1	1.93	18.2	1.13	19.3	1.08	—	—	—	—	1.5
4-Chloro	0.227	0.114	—	—	—	—	5.81	1.57	16.7	2.08	14.2	2.32	26.6	1.99	—	—	—	—	2.0
4-Bromo	0.232	0.15	—	—	—	—	4.82	1.75	16.7	1.89	14.3	2.33	—	—	—	—	—	—	2.0

[a] Taken as pH measured in 1:1 buffer solutions ($r = 0.50$). [b] Statistical parameters. [c] /dm^3 mol^{-1} s^{-1}. [d] /10^7 dm^3 mol^{-1} s^{-1}. [e] 2-Amino-2-(hydroxymethyl)propane-1,3-diol. [f] Estimated value. [g] Average of single values obtained for each catalyst.

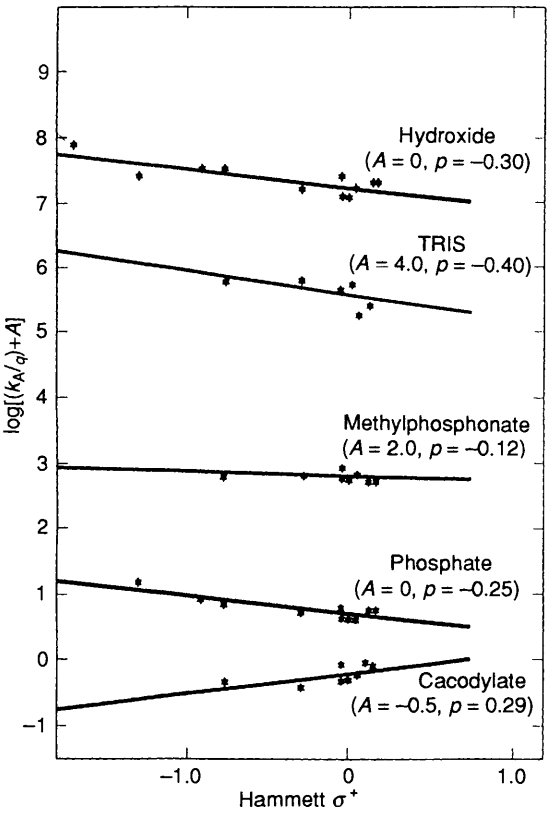

Fig. 3 Hammett plots for the base-catalysed breakdown of a series of aryl-substituted acetophenone methyl acetals; data taken from Table 3

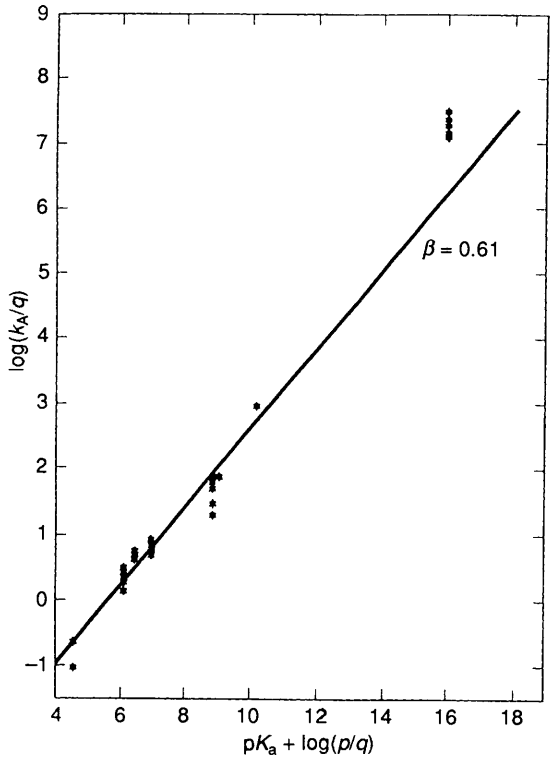

Fig. 4 Common Brønsted plot for the base-catalysed breakdown of a series of aryl-substituted acetophenone methyl acetals; data taken from Table 3

plot includes points for all substrates (apart from those for 4-dimethylamino, 4-amino and 4-hydroxy) and, again, the set of catalytic data is not sufficiently accurate to provide a meaningful Brønsted β value for each substrate. The situation

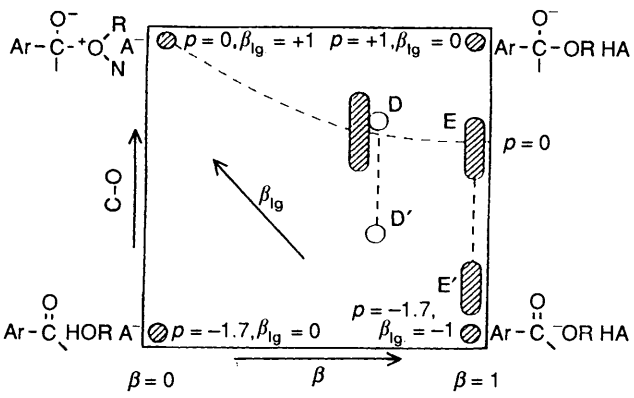

Fig. 5 Reaction coordinate diagram for the class n concerted base-catalysed breakdown of a series of aryl-substituted acetophenone methyl hemiacetals; for notations see the text. The numerical values of the various correlation coefficients are taken from ref. 27(*g*).

is further complicated by the fact that bases of different charge type are used. The least-squares line shown in Fig. 4 is drawn without the points for hydroxide ($\beta = 0.61$, correlation coefficient = 0.986). Although points for hydroxide catalysis usually show positive deviation from a plot based on general bases, a slightly better plot is actually obtained if hydroxide is included in this case ($\beta = 0.69$, correlation coefficient = 0.994). Both β values are of the right order of magnitude compared with $\beta = 0.66$–0.72 for the general-base-catalysed decomposition of α-bromoacetophenone hemiacetals.[20a]

All experimental indications so far have convinced us that the general-base-catalysed breakdown of aryl-substituted acetophenone methyl hemiacetals takes place by the usual class n concerted mechanism[26] according to Scheme 4.

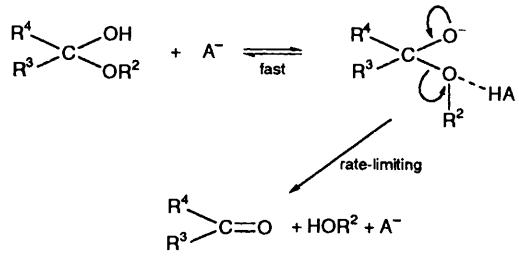

Scheme 4

In this reaction scheme the hemiacetal anion undergoes rate-limiting breakdown catalysed by the acid component of the buffer. In terms of a reaction coordinate diagram with C–O bond breakage and proton transfer coordinates as shown in Fig. 5, the observed substituent effects are explained by transition states located in the shaded area near D in the central part of the diagram ($\rho \approx 0$, $\beta \approx 0.6$, the pre-equilibrium step of Scheme 4 is taken into account by assigning a ρ value of +1 to the upper right-hand corner in Fig. 5). One assumption that is required in locating the positions of the transition states based on ρ values is that ρ varies in a linear fashion with the other reaction coordinates. This, however, can be shown in the present case to be inconsistent with the transition states located on the basis of β_{lg} values ($\beta_{lg} = d\log k_A/dpK_{lg}$ is measured along the diagonal in Fig. 5). Although β_{lg} has not been determined in our actual case, ρ and β_{lg}, as well as Brønsted β, are known for a very closely related study of the general-base-catalysed breakdown of α-bromoacetophenone hemiacetals.[20c] The locations D and D′ in Fig. 5 represent transition states based on ρ and β_{lg}, respectively, from this work. Similarly, in Fig. 5, E and E′ represent several aromatic systems involving OH^- as the catalyst,[27] with E the transition state location using ρ, E′ using β_{lg}.

We think our aromatic hemiacetal decomposition reaction offers a case of non-perfect synchronization[28] or imbalance in the transition state between the extent of C–O bond breakage and electronic reorganization, *i.e.*, a nonlinear response between Hammett ρ and other reaction coordinates. One simple interpretation is that in the breakdown direction there is considerable C–O bond breakage in the transition state as measured by β_{lg}, but the change in hybridization of the central carbon ($sp^3 \longrightarrow sp^2$), as measured by ρ, lags behind so that there is less interaction with the aromatic substituents in the transition state.

Unfortunately, the acetophenone system is not experimentally ideal for a further, more detailed investigation of this imbalance. As an alternative, but closely related, system we are now currently studying the breakdown of benzaldehyde hemiacetals, applying the double-mixing stopped-flow experimental technique of the present work.[29] The build-up of hemiacetal is considerably larger here, leading to much bigger amplitudes in the kinetic runs. In addition to studying the specific phenomenon of imbalance, we are currently interested in the general nature of concerted acid–base catalysis. In particular, we would like to be able to interpret the aromatic substituent effects for concerted general-base catalysis (Hammett plots in Fig. 3) in terms of detailed transition-state structures. This type of analysis has been made by Jencks and co-workers for a few non-aromatic carbonyl addition reactions, but requires large bodies of rather accurate kinetic data.[30]

Acknowledgements

This research was supported by a NATO Collaborative Research Grant (CRG 900990).

References

1 (*a*) T. H. Fife, *Acc. Chem. Res.*, 1972, **5**, 264; (*b*) E. H. Cordes and H. G. Bull, *Chem. Rev.*, 1974, **5**, 581.
2 (*a*) P. R. Young and W. P. Jencks, *J. Am. Chem. Soc.*, 1977, **99**, 8238; (*b*) R. A. McClelland and M. Ahmad, *J. Am. Chem. Soc.*, 1978, **100**, 7031; (*c*) T. L. Amyes and W. P. Jencks, *J. Am. Chem. Soc.*, 1989, **111**, 7888, 7900.
3 B. Capon, K. Nimmo and G. L. Reid, *J. Chem. Soc., Chem. Commun.*, 1976, 871.
4 (*a*) T. H. Fife and E. Anderson, *J. Am. Chem. Soc.*, 1971, **93**, 6610; (*b*) T. J. Przystas and T. H. Fife, *J. Am. Chem. Soc.*, 1980, **102**, 4391.
5 (*a*) A. L. Mori, M. A. Porzio and L. L. Schaleger, *J. Am. Chem. Soc.*, 1972, **94**, 5034; (*b*) A. L. Mori and L. L. Schaleger, *J. Am. Chem. Soc.*, 1972, **94**, 5039; (*c*) R. F. Atkinson and T. C. Bruice, *J. Am. Chem. Soc.*, 1974, **96**, 819.
6 R. A. McClelland and N. E. Seaman, *Can. J. Chem.*, 1987, **65**, 1689.
7 B. Capon, *Pure Appl. Chem.*, 1977, **49**, 1001; (*b*) J. L. Jensen, A. B. Martinez and C. L. Shimazu, *J. Org. Chem.*, 1983, **48**, 4175.
8 J. L. Jensen and P. A. Lenz, *J. Am. Chem. Soc.*, 1978, **100**, 1291.
9 R. L. Finley, D. G. Kubler and R. A. McClelland, *J. Org. Chem.*, 1980, **45**, 644.
10 R. A. McClelland and P. E. Sørensen, *Acta Chem. Scand.*, 1990, **44**, 1082.
11 Slightly modified version of the procedure for synthesising aryl-substituted acetophenone diethyl acetal, as described by (*a*) S. R. Sandler and W. Karo, *Organic Functional Group Preparations, Organic Chemistry*, eds. A. T. Blomquist and H. Wasserman, Academic Press, New York, 1972, vol. III; (*b*) C. E. Kaslow and W. R. Lawton, *J. Am. Chem. Soc.*, 1950, **72**, 1723; (*c*) T. S. Davis, P. D. Feil, D. G. Kubler and D. J. Wells, *J. Org. Chem.*, 1975, **40**, 1478; (*d*) G. M. Loudon, C. K. Smith and S. E. Zimmerman, *J. Am. Chem. Soc.*, 1974, **96**, 465.
12 (*a*) L. Claisen, *Ber. Dtsch. Chem. Ges.*, 1898, **31**, 1012; (*b*) M. T. Bogert and P. P. Herrera, *J. Am. Chem. Soc.*, 1923, **45**, 238; (*c*) R. Taylor, *J. Chem. Soc., Perkin Trans. 2*, 1988, 737; (*d*) R. A. McClelland, B. Watada and C. S. Q. Lew, *J. Chem. Soc., Perkin Trans. 2*, 1993, 1723.
13 (*a*) J. Touillec and E.-A. Mohiedine, *Anal. Chim. Acta*, 1979, **109**, 187; (*b*) J. Touillec, personal communication; (*c*) J. Touillec, M. El-Alaoui and P. Kleffert, *J. Org. Chem.*, 1983, **48**, 4808.
14 *Sadtler Standard Spectra*, Sadtler Research Laboratory, Division of Bio-Rad Laboratory, Inc., Researchers, Philadelphia, 1980, Supplement 1989.
15 U. Lienhard, H. P. Fahrni and M. Neuenschwander, *Helv. Chim. Acta*, 1978, **61**, 1615.
16 H. Staudinger and A. Kon, *Ann. Chem.*, 1911, **384**, 111.
17 N. M. Rodigin and E. N. Rodigina, *Consecutive Chemical Reactions, Mathematical Analysis and Development*, van Nostrand, Princeton, 1964.
18 On-Line Instrument Systems Inc., Route 2, Jefferson, GA 30549, USA.
19 B. Capon and M. C. Smith, *J. Chem. Soc B*, 1969, 1031.
20 (*a*) P. E. Sørensen, K. J. Pedersen, P. R. Pedersen, V. M. Kanagasabapathy and R. A. McClelland, *J. Am. Chem. Soc.*, 1988, **110**, 5118; (*b*) B. G. Cox, A. J. Kresge and P. E. Sørensen, *Acta Chem. Scand., Ser. A*, 1988, **42**, 202; (*c*) P. E. Sørensen, T. Løgager, V. M. Kanagasabapathy and R. A. McClelland, *Bull. Soc. Chim. France*, 1988, 313; (*d*) T. J. Przystas and T. H. Fife, *J. Am. Chem. Soc.*, 1981, **103**, 4884.
21 MicroMath Scientific Software, PO Box 21550, Salt Lake City, Utah 84121, USA.
22 K. A. Connors, *Chemical Kinetics. The Study of Reaction Rates in Solution*, VCH, New York, 1990.
23 Y. Yukawa and Y. Tsuno, *Bull. Chem. Soc. Jpn.*, 1959, **32**, 965.
24 G. M. Louden and C. Berke, *J. Am. Chem. Soc.*, 1974, **96**, 4508.
25 (*a*) H. van Bekkum, P. E. Verkade and B. M. Wepster, *Recl. Trav. Chim.*, 1959, **78**, 815; (*b*) R. W. Taft, Jr., *J. Phys. Chem.*, 1960, **64**, 1805.
26 W. P. Jencks, *Acc. Chem. Res.*, 1976, **9**, 425.
27 (*a*) R. P. Bell and P. E. Sørensen, *J. Chem. Soc., Perkin Trans. 2*, 1976, 1594; (*b*) M. Arora, B. G. Cox and P. E. Sørensen, *J. Chem. Soc., Perkin Trans. 2*, 1979, 103; (*c*) D. J. Hupe and W. P. Jencks, *J. Am. Chem. Soc.*, 1977, **99**, 451; (*d*) J. M. Sayer and W. P. Jencks, *J. Am. Chem. Soc.*, 1977, **99**, 464; (*e*) D. J. Hupe and D. Wu, *J. Am. Chem. Soc.*, 1977, **99**, 7653; (*f*) D. J. Hupe, D. Wu and P. Shepperd, *J. Am. Chem. Soc.*, 1977, **99**, 7659; (*g*) R. A. McClelland and M. Coe, *J. Am. Chem. Soc.*, 1983, **105**, 2718.
28 C. F. Bernasconi, *Acc. Chem. Res.*, 1992, **25**, 9; *Adv. Phys. Org. Chem.*, 1992, **27**, 119.
29 A preliminary account was presented at the *Toronto International Conference on Organic Reactive Intermediates*, Scarborough Campus, University of Toronto, Toronto, Canada, July–August, 1992.
30 (*a*) L. H. Funderburk, L. Aldwin and W. P. Jencks, *J. Am. Chem. Soc.*, 1978, **100**, 5444; (*b*) P. E. Sørensen and W. P. Jencks, *J. Am. Chem. Soc.*, 1987, **109**, 4675.

Paper 4/02279C
Received 18*th April* 1994
Accepted 30*th June* 1994